Engineering Structures 81 (2014) 256–264

Contents lists available at ScienceDirect

Engineering Structures

journal homepage: www.elsevier.com/locate/engstruct

Integrated structure-passive control design of linear structures under seismic excitations

O. Curadelli *, M. Amani

Laboratory of Experimental Dynamic, National University of Cuyo, CONICET, Centro Universitario, Parque Gral. San Martín, 5501 Mendoza, Argentina

A R T I C L E   I N F O

Article history:
Received 9 November 2013
Revised 30 September 2014
Accepted 1 October 2014

Keywords:
Integrated design
Optimal design
Passive energy dissipation system

A B S T R A C T

For purpose of enhancing the seismic performance of civil structures, external passive energy dissipation systems have been extensively used. Usually, the energy dissipation system is provided once the structure has been designed. Obviously, a sequential procedure cannot lead to the best overall design. In this paper, a simultaneous integrated design of the structure and passive control system is formulated as a two-objective optimization problem. As in almost all optimization problems with conflicting objective functions, in this study, different optimal solutions (efficient designs) that meet required restrictions are obtained. Since, the stochastic structural response is obtained in the frequency domain from the power spectral density function of the excitation, the proposed approach is very efficient, robust and requires considerably less computational effort than time history analysis. The methodology is demonstrated through a numerical example on a shear-type framed building.

1. Introduction

For purpose of enhancing the seismic performance of civil structures, external passive energy dissipation systems have been extensively used [1,2]. Traditionally, the process of designing a structure and its passive vibration control system has been sequential and obviously it cannot lead to the best overall design. In general, an energy dissipation system is optimally designed to improve the seismic performance after the structure has been initially designed under constraints on weigh, strength and displacements [3,4]. However, because of the coupling between the structure and control system, a simultaneous integrated design of both leads to a better performance (optimal solution) than a sequential design [5–7]. Reyer [6] formally classified the various optimization strategies into sequential, iterative, bi-level (nested), and simultaneous. A comparison between those strategies was also conducted by the author. Early works regarding sequential design were conducted by Khot et al. [8], and Venkayya and Tischler [9]. To improve the optimality level of sequential strategies, Grigiriadis et al. [10] and Smith et al. [11] proposed iterative strategies which consist of first, improving the structure design without compromising the control performance then, optimizing the controller without compromising the structural performance and so on until the tolerance is reached. Bi-level strategies are based on two nested optimization loops. The outer loop optimizes a scalar objective function which is a linear combination of two objective functions, one related to the structure and the other one to the controller, by varying only the structural design. In the inner loop an optimal controller for each structure selected by the outer loop is generated [12,13]. Finally, simultaneous optimization involves finding the optimal system design by solving the same scalar objective function of the previous case, but changing the design parameters of both structure and controller [14–17]. This strategy usually involves a complex non-convex mathematical problem. Fathy et al. [18] showed rigorously that system-level optimally is guaranteed with the nested and simultaneous strategies, but not with the sequential o iterative strategies. In the aerospace industry, integrated optimal design of structural-control systems has had a great development in the last 30 years as is evident from previous references; however, in civil engineering applications, there is still a widespread resort to traditional (sequential) design [19–21]. Most woks in the literature address the integrated design of the structure combined with an active control system and only a few with a passive control system. A simultaneous integrated design of the structure-control system from a composite objective function introduced as a linear combination of structural and active control objective functions was presented by Salama et al. [22]. A formal optimization procedure has been developed by Chattopadhyay and Seeley [23] which addresses the optimal locations of piezoelectric actuators and structural parameters. An algorithm used to minimize multiple and conflicting

* Corresponding author at: Lamadrid 3430, Godoy Cruz, 5547 Mendoza, Argentina. Tel.: +54 0261 4135000 2195; fax: +54 0261 4380120.
E-mail address: ocuradelli@fing.uncu.edu.ar (O. Curadelli).

http://dx.doi.org/10.1016/j.engstruct.2014.10.002
0141-0296/

objective functions associated with the coupled design of both, structure and active control system is introduced by Cheng [24]. On two structural design examples, Pareto optimal solutions were obtained. Rao et al. [25] presented a procedure similar to that Cheng [24], but applied on two truss structures. Khot [26] proposed a method to simultaneously design structure-control system to suppress structural vibrations due to external disturbances using a multi-objective optimization approach based on global criteria. A two-stage procedure for a controlled structural system design was presented by Cimellaro et al. [27]. The methodology is based on a redesign of the structure for better controllability by modifying the linear structural system (mass, stiffness and damping) and reducing the active control power. Similar approach, but applied to inelastic structures is described in Cimellaro et al. [28].

Few researchers treated the problem that simultaneously evaluates stiffness and added passive damping of linear structural systems subjected to seismic o random excitations. Takewaki [29] introduce a design problem to minimize the sum of relative story displacements to stationary random excitation subjected to a constraint on the sum of the stiffness and damping coefficients. Park et al. [30] described an approach for an integrated optimal design of a viscoelastically damped structural system. Optimization problem is formulated adopting as design variables, the amount and locations of the viscoelastic dampers. To solve the optimization problem, a genetic algorithm is used as a numerical searching technique. On the other hand, Cimellaro [31] proposed a procedure based on a generalized objective function defined by a linear combination of the norm of displacement, acceleration and base shear transfer functions evaluated at the updated fundamental natural frequency constrained by the total stiffness and damping.

For providing assistance to the structural engineer (decision-maker), in the present work, a simultaneous integrated design of the structure and passive control system formulated as a two-objective optimization problem is proposed. The outstanding point of the procedure described in the study is to have chosen the total story stiffness and the total story damping as conflicting-objective functions. In general, by reducing stiffness, the absolute acceleration and consequently the base shear decrease, but at the expense of an increase in the displacements; on the other hand, by increasing the energy dissipation, the relative displacements are reduced with little or no increase in the absolute acceleration [31,32]. Thus, the procedure gives a broad overview of different Pareto-optimal solutions (designs) that meet a required structural performance, and enables to select the best compromise solution as a trade-off between stiffness and added damping. Knowing that the main contribution to the total uncertainty is due to the excitation and with the aim of achieving robust results, the most appropriate approach to model the excitation is through a stationary stochastic process characterized by a power spectral density function compatible with the response spectrum defined by the seismic code provisions. Since the maximum structural response is estimated in the frequency domain through stochastic vibration theory, this approach is more efficiently and requires considerably less computational effort than time history analysis. From the results on a symmetrical building modelled as a linear shear-type planar frame it is found that through the proposed procedure, different efficient designs can be reached maintaining the required level of structural performance.

2. Formulation of the integrated design problem

As mentioned before, the integrated design problem of the structure and the passive control system is formulated as a two-objective optimization problem expressed as follows:

Find $\boldsymbol{z}$ that minimizes the following objective function vector:

$$\boldsymbol{f}(\boldsymbol{z}) = \{f_1(\boldsymbol{z}), f_2(\boldsymbol{z})\} \tag{1}$$

subjected to

$$g_i(\boldsymbol{z}) \leqslant 0, \quad i = 1, 2, \ldots, p$$

$$u_i(\boldsymbol{z}) = 0, \quad i = 1, 2, \ldots, q$$

in which $\boldsymbol{z}$ is the design variable vector, $f_1(\boldsymbol{z}), f_2(\boldsymbol{z})$ are the objective functions and $g_i(\boldsymbol{z})$, $u_i(\boldsymbol{z})$ are the constraint functions.

The main characteristic of the two-objective optimization problem is that none of the feasible solutions allow simultaneously minimizing both objective functions. To overcome this problem a Pareto-optimal solution is useful and defined as [33]: if vector $\boldsymbol{z}^p$ is a solution of Eq. (1), there exists no feasible vector $\boldsymbol{z}$ that would decrease same objective function without causing a simultaneous increase in, at least, other objective function. Usually several Pareto-optimal solutions exist for a vector optimization problem and to select the best solution, the designer judgment alongside additional information are needed. There are several methods for solving a vector optimization problem. The most commonly used approach, known as the weighting method, substitutes the vector optimization problem Eq. (1) into a scalar one formulated as a weighted sum of the individual objective functions as:

$$F(\boldsymbol{z}) = w_1 f_1(\boldsymbol{z}) + w_2 f_2(\boldsymbol{z}) \tag{2}$$

in which w_1 and w_2 are weighting factors.

A set of Pareto-optimal solutions denoted as $\{\boldsymbol{z^p}\}$ can be generated by varying the weight of each objective function. In order to select the best solution, the designer should previously define the weight of each objective function from additional information (cost, feasibility, etc.), or resort to a decision-making process [34,35]. In this study, besides displaying the set of Pareto-optimal solutions, the following decision-making process is adopted. In a cooperative optimization procedure, the best solution should guarantee that each objective function reaches the lowest possible value, even if it is not its own minimum value. For this, an optimal solution $\boldsymbol{z_k}^*(k = 1,\ 2)$ minimizing ***individually*** to each objective function is obtained subjected to the constraints stated in Eq. (1). Then, a matrix $\boldsymbol{P}$ can be constructed as:

$$\boldsymbol{P} = \begin{bmatrix} f_1(\boldsymbol{z}_1^*) & f_2(\boldsymbol{z}_1^*) \\ f_1(\boldsymbol{z}_2^*) & f_2(\boldsymbol{z}_2^*) \end{bmatrix} \tag{3}$$

in which, the lowest values of each objective functions, $f_{k,min} = f_k(\boldsymbol{z}_k^*)$, are in the diagonal elements of matrix $\boldsymbol{P}$ and the highest ones outside of it, $f_{k,max} = max[f_k(\boldsymbol{z}_j^*)],\ k \neq j\ k,\ j = 1, 2$. During cooperative optimization, the *k-th* objective function should never have a value lower than $f_{k,min}$ (if the problem is well-defined), nor should it exceed $f_{k,min}$ (it runs counter to the objective of minimizing f_k). Based on these assertions, the following objective function can be constructed:

$$R = \prod_{k=1}^{2} \frac{[f_{k,max} - f_k(\boldsymbol{z^p})]}{[f_{k,max} - f_{k,min}]} \tag{4}$$

in which, the range of R is $0 < R < 1$ and $\boldsymbol{z^p}$ denotes a Pareto-optimal solution minimizes to Eq. (2).

Therefore the solution $\hat{\boldsymbol{z}}$ selected from Pareto-optimal set, $\{\boldsymbol{z^p}\}$, which maximizes R, is the best solution (rational compromise solution).

2.1. Objective functions and constraints

In any structural design, the aim is to guarantee a required level of structural performance at the lowest possible total cost. Assuming that non-structural live and dead floor masses are defined by operational requirements, the total cost is associated with the structural stiffness and the size of energy dissipation system. Without limiting the applicability of the methodology to any type of structure, a shear-type building is assumed as example in which, the stiffness and damping coefficients of each story are chosen as design variables grouped into a design vector, $\boldsymbol{z} = \{k_1, k_2, \ldots, k_n, c_1, c_2, \ldots, c_n\}^T$. Because the required level of performance can be achieved through a trade-off between the total story stiffness and the total story damping, the conflicting-objective functions are defined respectively as:

$$f_1(\boldsymbol{z}) = \sum_{i=1}^{n} k_i$$

$$f_2(\boldsymbol{z}) = \sum_{i=1}^{n} c_i \quad i = 1, 2 \ldots n \tag{5}$$

in which k_i and c_i are the stiffness and damping coefficients of the i-th story and n denotes the number of stories.

Constraint conditions may include displacements, stresses, frequencies, bucking loads, as well as upper and lower bounds of the design variables. In the present study the following constraint conditions are adopted:

$$\delta_{max} \leqslant \delta_l, \quad 0 \leqslant c_i, \quad k_l \leqslant k_i, \quad \xi_1 \leqslant \xi_l \tag{6}$$

in which c_i, k_i, are the damping and stiffness coefficients of the i-th story of the optimized structure (design variables, see Eq. (5)); δ_{max} is the mean peak of the maximum inter-story drift determined from Eq. (27);k_l and δ_l, are the story stiffness lower limit and the inter-story drift upper limit required by the structural performance criterion (Eq. (33)); ξ_i and ξ_j are the damping ratio of the fundamental vibrational mode of the optimized structure and the upper limit required by design.

3. Seismic ground excitation

Usually, studies on design of energy dissipation systems are carried out in time domain through Monte Carlo simulation using a sufficient number of deterministic artificially generated records [36]. However, in optimization problems with high computational cost due to numerous iterations, an alternative simple method is required. Spectral analysis, conducted in frequency domain, is an attractive method in which, a power spectral density function (PSDF), rather than a collection of time histories, can be advantageously used for modelling the excitation.

3.1. Derivation of design spectrum compatible power spectral density function

It is known that earthquake excitation is inherently random and has a strong contribution to the total uncertainty of the seismic analysis, therefore, if the evolution of the frequency content with time can be neglected, the most appropriate approach to model the excitation is through a stationary stochastic process characterized by a power spectral density function (PSDF). In this study the earthquake excitation is assumed as a stationary Gaussian random process with zero mean represented by means of a design spectrum compatible PSDF. Following the methodology developed by Vanmarcke [37] cited in the work conducted by Giaralis and Spanos [38], the design spectrum compatible PSDF can be approximated by the following recursive equation:

$$G(\omega_j) = \frac{4\xi}{\omega_j \pi - 4\xi\omega_{j-1}} \left(\frac{S_a^2(\omega_j \xi)}{\eta_j^2(\omega_j, \xi)} - \Delta\omega \sum_{k=1}^{j-1} G(\omega_k) \right) \quad \omega_j > \omega_0 \tag{7}$$

in which $G(\omega_j)$ and $S_a(\omega_j \xi)$ are the one-sided PSDF and the median pseudo-acceleration response spectrum, respectively, at a specific frequency ω_j and $\xi = 0.05$ is the assumed damping ratio; $\Delta\omega$ is the frequency step in which the frequency range is discretized; the peak factor η_j is calculated by Eq. (8). Specifically, it represents the factor by which the rms value of the response of a SDOF oscillator must be multiplied to predict the level S_a below which the peak response of the oscillator will remain, with probability p, throughout the duration of the input process T_s. Herein, the following approximated semi-empirical formula for the calculation of the peak factor is adopted, which is known to be reasonably reliable for earthquake engineering applications [35]:

$$\eta_j = \sqrt{2 \ln \left\{ 2\upsilon_j \left[1 - \exp\left(-q_j^{1.2} \sqrt{\pi \ln(2\upsilon_j)} \right) \right] \right\}} \tag{8}$$

in which

$$\upsilon_j = \frac{T_s}{2\pi} \omega_j (-\ln p)^{-1} \tag{9}$$

and

$$q_j = \sqrt{1 - \frac{1}{1-\xi^2} \left(1 - \frac{2}{\pi} \tan^{-1} \frac{\xi}{\sqrt{1-\xi^2}} \right)} \tag{10}$$

Eqs. (9) and (10) are close form expressions derived for a white noise PSDF which has to be a priori assumed without knowledge of $G(\omega_j)$ when the peak factor is calculated by Eq. (8). T_s = 20 s is the duration assumed for the underlying stationary process; p = 0.5 is an appropriate probability assumed for the purposes of this study and ω_o = 0.36 rad/s denotes the lowest bound of the existence domain of Eq. (7) for a PSDF [36].

The power spectrum density estimation obtained by Eq. (7) can be improved via the following iterative scheme [37]:

$$G^{i+1}(\omega_j) = G^i(\omega_j) \left[\frac{S_a^t(\omega_j, \xi)}{S_a^i(\omega_j, \xi)} \right]^2 \tag{11}$$

in which $S_a^t(\omega_j, \xi)$ and $S_a^i(\omega_j, \xi)$ are the target design spectrum and the associated design spectrum estimated in the *i-th* iteration, respectively.

4. Evaluation of stochastic response

The equations governing the dynamic motion of the structure provided with added viscous dampers subjected to an earthquake excitation may be written in the matrix form as:

$$\mathbf{M}\ddot{\mathbf{x}}(t) + (\mathbf{C} + \mathbf{C_v})\dot{\mathbf{x}}(t) + \mathbf{K}\mathbf{x}(t) = -\mathbf{M}\mathbf{r}\ddot{x}_g(t) \tag{12}$$

where $\mathbf{M}$, $\mathbf{K}$ and $\mathbf{C}$ are the mass, stiffness and the damping matrices of size $n \times n$, respectively, the matrix of the added viscous damping is denoted by $\mathbf{C_v}$, $\mathbf{r}$ is the influence vector, $\ddot{x}_g(t)$ is the horizontal acceleration of ground motion and, $\ddot{\mathbf{x}}(t)$, $\dot{\mathbf{x}}(t)$ and $\mathbf{x}(t)$ are the generalized acceleration, velocity and displacement vectors, of size $n \times 1$ respectively, being n the number of degree of freedom.

Note that, the matrix $\mathbf{K}$ and $\mathbf{C_v}$ are defined through elements k_i and c_i respectively obtained from the optimization process and the connectivity matrices.

Eq. (12) can be written such as the following system of first-order differential equations:

$$\frac{d}{dt}\mathbf{y} = \mathbf{G}\,\mathbf{y} + \mathbf{w} \tag{13}$$

where $\mathbf{y}$ is the state vector of size $2n \times 1$

$$\mathbf{y} = \{\boldsymbol{x}^T \dot{\boldsymbol{x}}^T\}^T \tag{14}$$

$\mathbf{G}$ is the augmented system matrix of size $2n \times 2n$

$$\mathbf{G} = \begin{bmatrix} [\mathbf{0}] & [\mathbf{I}] \\ -\mathbf{M}^{-1}\mathbf{K} & -\mathbf{M}^{-1}(\mathbf{C} + \mathbf{C}_v) \end{bmatrix} \tag{15}$$

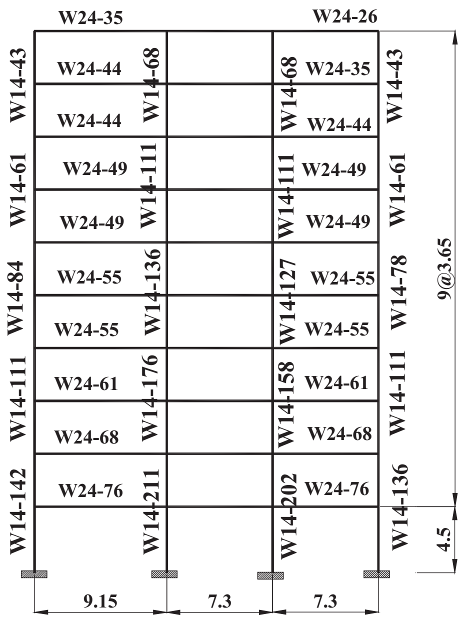

Fig. 1. Planar building frame (dimensions in m).

and **w** is the excitation vector of size $2n \times 1$

$$\mathbf{w} = -\{\{\mathbf{0}\} \quad \{\mathbf{1}\}\ddot{x}_0\}^T \tag{16}$$

where $\{\mathbf{0}\}$ and $\{\mathbf{1}\}$ denotes the null and unit vector, respectively, of size $1 \times n$; $[\mathbf{0}]$ and $[\mathbf{I}]$ denotes the null and identity matrix, respectively, of size $n \times n$; $\mathbf{M}^{-1}$ is the inverse of mass matrix $\mathbf{M}$, and $\ddot{x}_0(t)$ denotes the ground motion assumed as a zero-mean white noise random process with a PSDF of constant intensity, S_o.

Let the covariance matrix of **y** be **S** with

$$S_{ij} = E[y_i y_j] \tag{17}$$

in which $E[.]$ is the expectation operator and y_i is the *i-th* element of vector **y**.

It can be shown [35] that for a zero-mean white noise random process, **S** satisfies the following differential equation:

$$\frac{d}{dt}\mathbf{S} = \mathbf{G}\mathbf{S}^T + \mathbf{S}\mathbf{G}^T + \mathbf{D} \tag{18}$$

in which **D** is the covariance matrix between the state and excitation vectors of size $2n \times 2n$ and $D_{ij} = 0$ except that $D_{2n,2n} = 2\pi\, S_0$.

As the excitation is assumed stationary, **D** is time independent, then, the stationary solution of Eq. (18) can be obtained by solving the Lyapunov matrix equation:

$$\mathbf{G}\mathbf{S}^T + \mathbf{S}\mathbf{G}^T + \mathbf{D} = \mathbf{0} \tag{19}$$

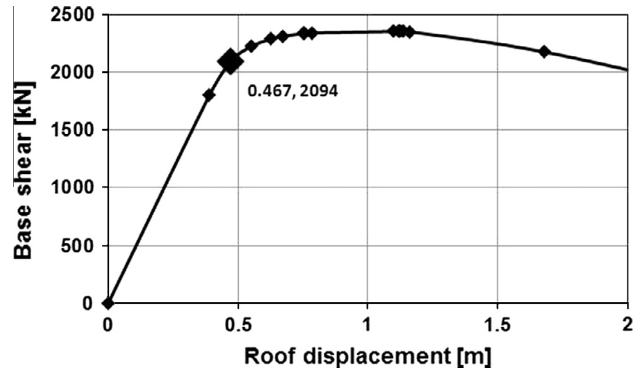

Fig. 3. Pushover of planar building frame.

It is important note that the previous stochastic response has been obtained from a white noise type excitation $\ddot{x}_0(t)$ with constant PSDF; however, the PSDF obtained by Eq. (11) which represents the stationary Gaussian random process, $\ddot{x}_g(t)$ is not constant over the frequency range. This obstacle can be circumvented by filtering the white noise $\ddot{x}_0(t)$ through two linear filters as follows:

$$\ddot{x}_g(t) + 2\xi_g\omega_g\dot{x}_g(t) + \omega_g^2 x_g(t) = -(\ddot{x}_f(t) + \ddot{x}_0(t)) \tag{20}$$

$$\ddot{x}_f(t) + 2\xi_f\omega_f\dot{x}_f(t) + \omega_f^2 x_f(t) = -\ddot{x}_0(t) \tag{21}$$

in which ω_g, ξ_g, ω_f and ξ_f are the ground filter parameters. Eqs. (20) and (21) lead to the Clough and Penzien stationary PSDF [39]:

$$G_{CP}(\omega_j) = S_0\left(\frac{1+4\xi_g^2(\omega_j/\omega_g)^2}{\left[1-(\omega_j/\omega_g)^2\right]^2+4\xi_g^2(\omega_j/\omega_g)^2}\right)\left(\frac{(\omega_j/\omega_f)^4}{\left[1-(\omega_j/\omega_f)^2\right]^2+4\xi_f^2(\omega_j/\omega_f)^2}\right) \tag{22}$$

Thus, to make compatible the PSDFs given by Eqs. (11) and (22), the filter parameter are estimated by fitting both functions.

On the basis of the above considerations, the stochastic structural response is obtained by solving the Eq. (19) in which, the state vector, **y**, the augmented system matrix, **G**, and excitation vector, **w**, can be re-written as follow:

$$\mathbf{y} = \{\mathbf{x}^T \quad \dot{\mathbf{x}}^T \quad x_f \quad \dot{x}_f \quad x_g \quad \dot{x}_g\}^T \tag{23}$$

$$\mathbf{G} = \begin{bmatrix} [0] & [I] & \{0\}^T & \{0\}^T & \{0\}^T & \{0\}^T \\ -\mathbf{M}^{-1}\mathbf{K} & -\mathbf{M}^{-1}(\mathbf{C}+\mathbf{C}_v) & -\{1\}^T\omega_f^2 & -\{1\}^T 2\xi_f\omega_f & \{1\}^T\omega_g^2 & \{1\}^T 2\xi_g\omega_g \\ \{0\} & \{0\} & 0 & 1 & 0 & 0 \\ \{0\} & \{0\} & -\omega_f^2 & -2\xi_f\omega_f & \omega_g^2 & 2\xi_g\omega_g \\ \{0\} & \{0\} & 0 & 0 & 0 & 1 \\ \{0\} & \{0\} & 0 & 0 & -\omega_g^2 & -2\xi_g\omega_g \end{bmatrix} \tag{24}$$

$$\mathbf{w} = \{\{0\} \quad \{0\} \quad 0 \quad 0 \quad 0 \quad -\ddot{x}_0\}^T \tag{25}$$

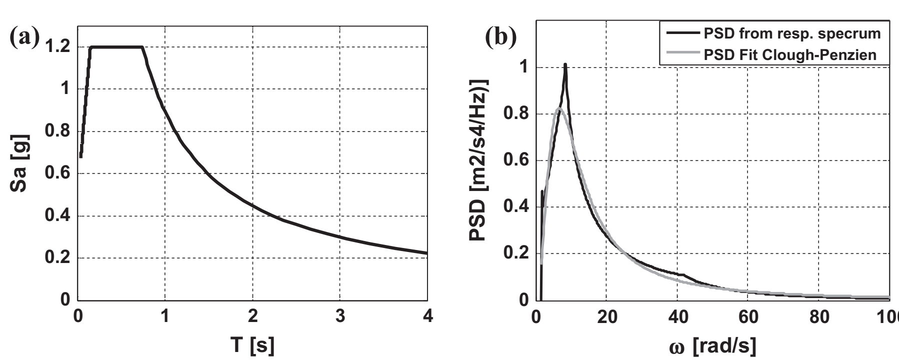

Fig. 2. (a) UBC 97, Pseudo-accel. resp. spectrum and (b) PSDF and Clough-Penzien model Fit.

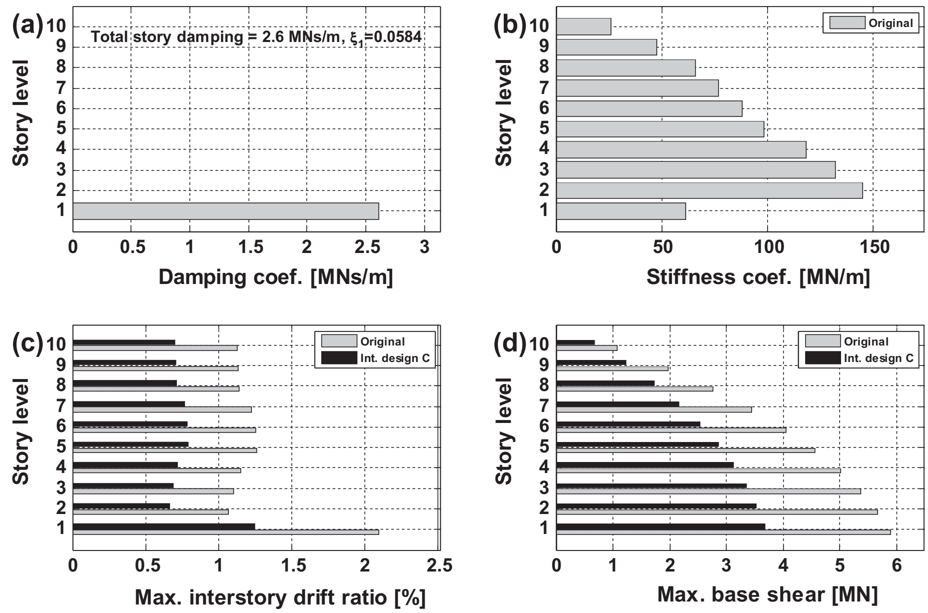

Fig. 4. Baseline case. (a) Optimal damping distribution, (b) stiffness distribution, (c) Max. inerstory drift ratio, (d) Max. base shear distribution.

and the elements of the covariance matrix **D** of size $2n + 4 \times 2n + 4$ are $D_{ij} = 0$ except that $D_{2n+4,2n+4} = 2\pi\, S_0$,.

Once the mean square value of structural response have been determined by Eq. (19) in matrix **S**, the standard deviation vector of the inter-story drift can be obtained as [40]:

$$\boldsymbol{\sigma}_{\mathbf{d}} = \{\sigma_i\} = diag(\mathbf{T}\,\mathbf{S}\,\mathbf{T}^T)^{1/2} \quad i = 1, 2 \ldots n \tag{26}$$

in which **T** is a constant matrix consisting of 1, −1 and 0.

The mean peak of the maximum inter-story drift needed in Eq. (6) can be calculated from the standard deviation value determined by Eq. (26) as follows [41]:

$$\delta_{max} = p_f \sigma_{max} \tag{27}$$

$$p_f = \sqrt{2 \ln v_e T_s} + \frac{0.5775}{\sqrt{2 \ln v_e T_s}} \tag{28}$$

in which δ_{max} is the mean peak of the maximum inter-story drift (Eq. (6)), σ_{max} is the maximum value of the inter-story drift vector (Eq. (26)), p_f is the peak factor, v_e is the modified mean zero-crossing rate, and T_s is the time duration of the excitation. Der Kiureghian [40] derived a simple expression for v_e from a SDOF subjected to white noise ground acceleration given by:

$$v_e = \begin{cases} (1.90\xi^{0.15} - 0.73)\,v, & (\xi < 0.54) \\ v, & (\xi \geqslant 0.54) \end{cases} \tag{29}$$

where

$$v = \frac{\omega_1}{\pi} \tag{30}$$

in which v is the zero-crossing rate of the response, and ω_1 and ξ are the natural frequency and the damping ratio of the SDOF structure, respectively. For multi-degree-of-freedom (MDOF) structures, both parameters which correspond to the fundamental vibration mode are used under the assumption that the fundamental mode dominates the dynamic response.

Damping ratio ξ_k of *k-th* mode needed in Eq. (6) can be obtained from the complex conjugate eigenvalues of matrix **G** as:

$$\xi_k = -\frac{\alpha_k}{\sqrt{\alpha_k^2 + \omega_k^2}} \tag{31}$$

in which the complex conjugate pairs of eigenvalues of **G** are given by:

$$\lambda_k = \alpha_k \pm j\omega_k \quad k = 1, 2 \ldots m \tag{32}$$

where m is the number of modes and $j = \sqrt{-1}$.

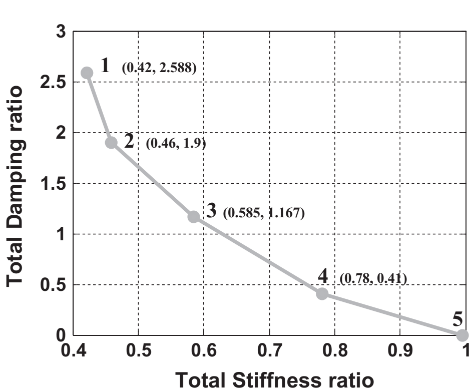

Fig. 5. Pareto-optimal solutions (different combinations of total story stiffness and total story damping).

5. Numerical example

5.1. Example: 10 story planar building frame

The example consists of the three bays, 10-stories high steel frame, in a building with two planes of symmetry and with a regular stiffness distribution in height. As reported in Ref. [42], the structure was designed for a PGA of 0.5 g (value from seismic hazard curve that has a 2% chance of exceedance in 50 years) in accordance with the provisions of the UBC [43]. The total mass per floor is 47 t and it is assumed a Young's modulus of steel E = 200 GPa, resulting in a fundamental period for low amplitude vibration equal to T_1 = 1.67 s. The internal damping was assumed

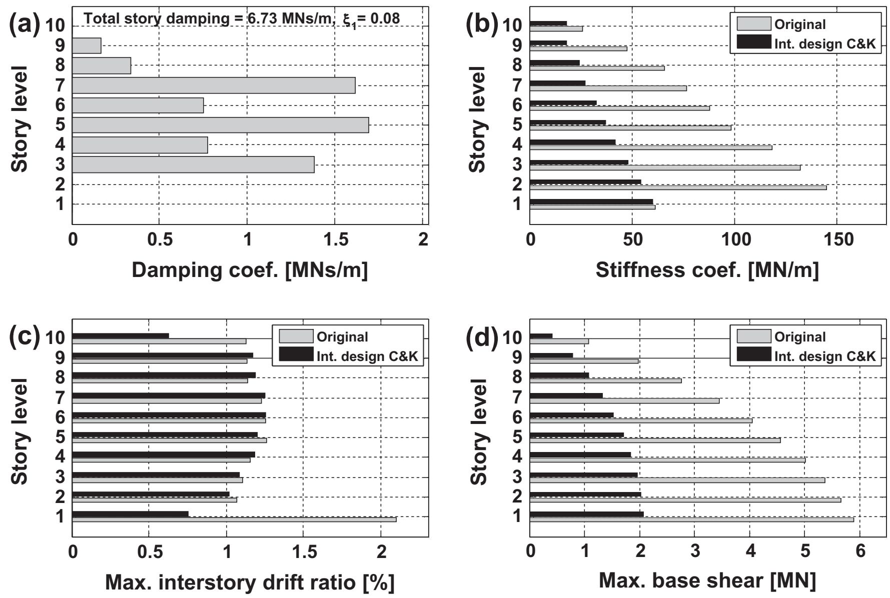

Fig. 6. Structural variables from Pareto-optimal solution 1.

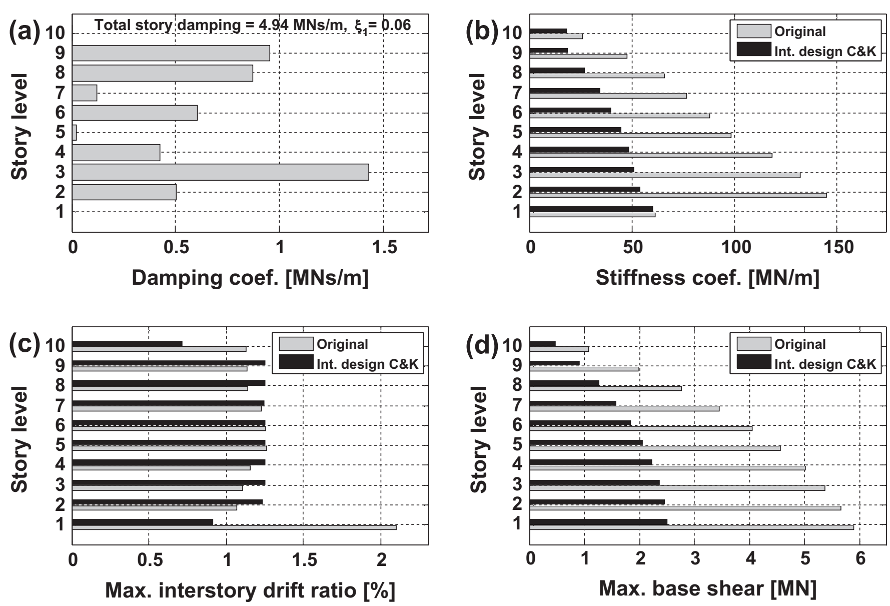

Fig. 7. Structural variables from Pareto-optimal solution 2.

to be 2% of critical damping ratio for all modes. Without loss of generality and for the sake of simplicity, an equivalent shear-type model of the original frame (Fig. 1) is defined by minimizing the differences in the modal parameters between both, model and structure.

5.2. Excitation and constraint conditions

The excitation (Fig. 2a) was defined from the UBC [43] pseudo-acceleration response spectrum for seismic zone $Z = 0.4$, soil profile type SC, and seismic source type A, with closest distance to known seismic source equal to 5 km. In Fig. 2b the corresponding compatible PSDF obtained by Eq. (11) (dashed line) and the Clough–Penzien approach (Eq. (22)) (continuous line) are displayed.

To meet the structural performance required, in this example the following constraint conditions (Eq. (6)) are assumed:

To ensure an overall linear structural behaviour, from a push-over analysis of the original structure (Fig. 3), the upper limit of the inter-story drift (maximum allowable inter-story drift) assumed constant was established as:

$$\delta_l = \theta h_i \tag{33}$$

With

$$\theta = \frac{\delta}{h} = 0.0125 \tag{34}$$

in which h_i is the *i-th* story height; $\boldsymbol{\theta}$ is the upper limit of the inter-story drift ratio; $\delta = 0.467$ m is the roof displacement at the elastic limit of the pushover curve (Fig. 3) and h is the building height.

– While the optimal constraint on the minimum stiffness is left to the professional judgment, without loss of generality in this study, the story stiffness lower limit, k_l (Eq. (6)), was determined from the original structure (without added damping)

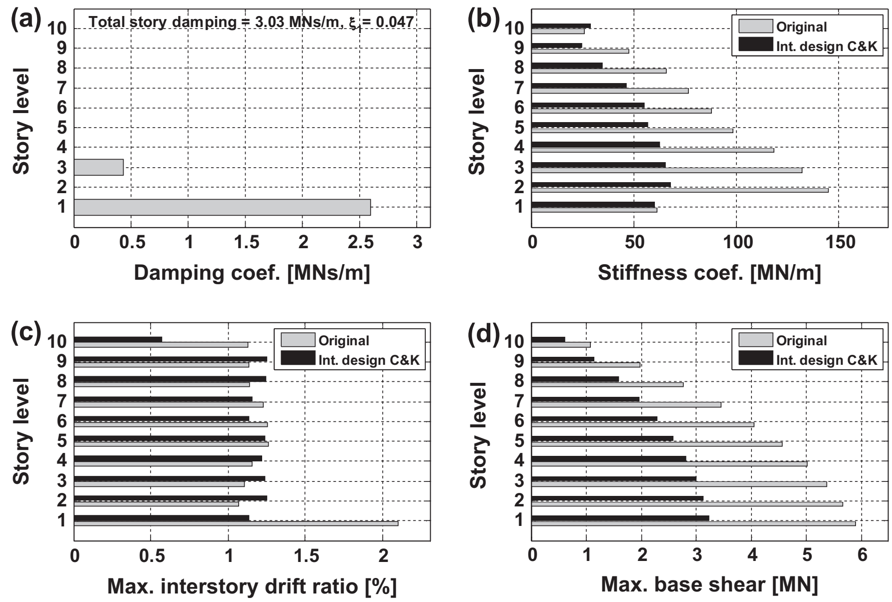

Fig. 8. Structural variables from Pareto-optimal solution 3.

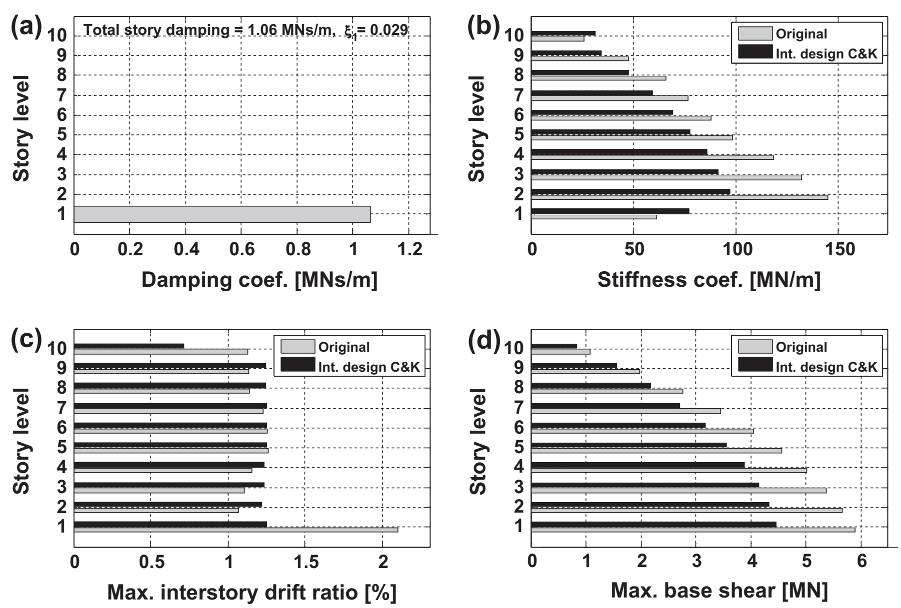

Fig. 9. Structural variables from Pareto-optimal solution 4.

as the minimum story stiffness that leads to the maximum inter-story drift allowable of $\delta_l = 0.0125h_i$ with an excitation that has a 10% chance of exceedance in 50 years.

– Without loss of generality, assuming that on the structure provided with added dampers the damping ratio of the fundamental mode was limited by design to 10%, it was necessary to impose the following condition $\xi_1 < 0.1$ on Eq. (6).

6. Discussion of results

As a baseline case, on the original structure (without changes in the stiffness) the total story damping to meet the required structural performance level (allowable inter-story drift, $\delta_l = 0.0125h_i$) is determined by the proposed methodology using only the objective function $f_2(z)$ (Eq. (5)). Fig. 4a shows the optimal distribution of story damping coefficients obtained on the structure with the original story stiffness distribution (Fig. 4b). In Fig. 4c–d can be observed that with a total story damping equal to 2.6 MNs/m ($\xi_1 = 0.0584$), the structural performance level on the maximum inter-story drift ($\delta_l = 0.0125h_i$) is reached at first story level and the base shear is reduced about 37.5% with respect to the original structure.

Only five representative Pareto-optimal solutions (i. e. designs with different combinations of story stiffnesses and story damping coefficients) generated by varying the weight of each objective function (Eq. (2)) that meet the previous constraint conditions (Section 5.2) are shown in Fig. 5. It should be noted that both, the total story stiffness and the total story damping obtained in each solution have been normalized with those values of the baseline case (Fig. 4) as follows:

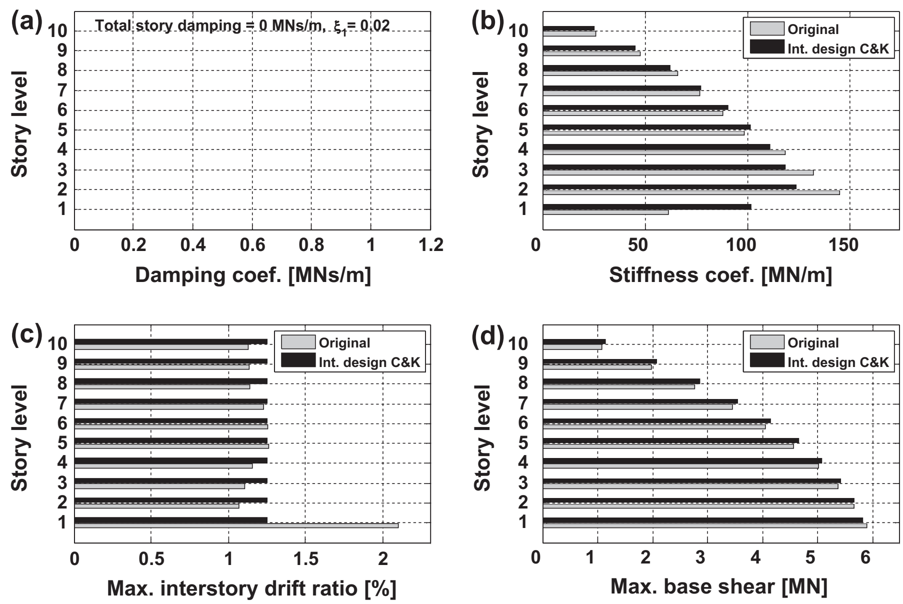

Fig. 10. Structural variables from Pareto-optimal solution 5.

$$\underline{K}^{j} = \frac{\left[\sum_{i=1}^{n} k_i\right]^{j}}{\left[\sum_{i=1}^{n} k_i\right]^{o}}$$

$$\underline{D}^{j} = \frac{\left[\sum_{i=1}^{n} c_i\right]^{j}}{\left[\sum_{i=1}^{n} c_i\right]^{o}} \quad j = 1, \ldots, 5 \quad i = 1, 2, \ldots, n \tag{35}$$

in which $\underline{K}^j$ and $\underline{D}^j$ are the total stiffness and damping ratio, respectively and superscript "j" refers to j-K Pareto-optimal solution and superscript "o" refers to baseline case (Fig. 4).

Optimal distributions of story damping coefficients, story stiffnesses, maximum inter-story drifts and maximum base shear obtained with the proposed methodology for each Pareto-optimal solution (Fig. 5) are displayed in Figs. 6–10, respectively.

The following observations can be made from the results presented in Figs. 6–10.

Solution 1 (Fig. 6) corresponds to the case in which the structure has the minimum permissible total story stiffness (42% of the total story stiffness of baseline case, $K^1 = 0.42$) and the largest total story damping (6.73 MNs/m, $D^1 = 2.59$). These quantities lead to the lowest maximum base shear (2.02 MN) with a maximum inter-story drift ratio equal to 1.25% at 6th and 7th story. On the other end of Pareto-optimal solution set (solution 5, Fig. 10), the total story stiffness is equal to that of the original structure (baseline case) but with an optimal distribution and the story drift is controlled without added damping. The distribution of base shear remains approximately unchanged. Solutions 2, 3 and 4 show intermediate results. In solutions 3 and 4 it is important to highlight the particular combination of total story stiffness and damping necessary to reach the structural performance ($\delta_l = 0.0125h_i$). From solution 3 (Fig. 8) can be observed that with a 17% increase on the total story damping of the baseline case (Fig. 5) ($\underline{D}^3 = 1.167$), the total story stiffness can be reduced approximately 40% ($\underline{K}^3 = 0.585$); while that in solution 4 (Fig. 9), the total story stiffness can be reduced 22% ($\underline{K}^4 = 0.78$) by installing a total story damping equal to 40% ($\underline{D}^4 = 0.41$) of that required in the baseline case (Fig. 5). It is important to highlight the uniform inter-story drift distribution that is attained in all solutions (1–5). Taking into account additional information, the designer will decide which solution will be the best for each application. Using the decision-making process (Eq. (4)), the solution 3 is the best solution which leads to the maximum value of R.

7. Conclusions

In the present work, a simultaneous integrated design of the structure and the passive control system is formulated as a two-objective optimization problem. The main characteristic of the proposed procedure is to have chosen the total story stiffness and the total story damping as conflicting-objective functions. Thus, the methodology gives a broad overview of different Pareto-optimal solutions that meet a required structural performance and enables to decision-maker to select the best compromise solution. This solution represents the maximum benefit that can be obtained from both objectives stated in the optimization problem resulting in an efficient and well-balanced structural design.

The proposed approach is very efficient, robust and requires considerably less computational effort than time history analysis since the stochastic structural response is estimated, from the power spectral density function that characterizes the excitation, in the frequency domain. Moreover, in the expectation of a better overall design, the weighting method can be easily extended to more than two conflicting objective functions (multi-objective formulation) and several constraint conditions, but with higher computational costs.

Numerical results, obtained from a symmetrical building modelled as a linear shear-type planar frame, showed that with the proposed integrated procedure, different efficient alternative designs can be reached maintaining the required level of structural performance.

Acknowledgements

The authors gratefully acknowledge the financial support of CONICET and National University of Cuyo, Argentina.

Appendix A. Supplementary material

Supplementary data associated with this article can be found, in the online version, at http://dx.doi.org/10.1016/j.engstruct.2014.10.002.

References

[1] Soong TT, Dargush GF. Passive energy dissipation systems in structural engineering. 1st ed. New York: John Wiley & Sons; 1997.
[2] Curadelli RO, Riera JD. Design and testing of a lead damper for seismic applications. Proc IMechEngng Part C: J Mech Eng Sci 2006;221:159–65.
[3] Aydin E, Boduroglu MH, Guney D. Optimal damper distribution for seismic rehabilitation of planar building structures. Eng Struct 2007;29:176–85.
[4] Martínez M, Curadelli O, Compagnoni ME. Optimal design of passive viscous damping systems for buildings under seismic excitation. J Const Steel Res 2013;90:253–64.
[5] Haftka RT. Integrated structure-control optimization of space structures. AIAA 1990:CP-90-1190.
[6] Reyer JA. Combined embodiment design and control optimization: effect of cross-disciplinary coupling. PhD dissertation, at The University of Michigan; 2000.
[7] Peters DL. Coupling and controllability in optimal design and control. PhD dissertation, at The University of Michigan; 2010.
[8] Khot NS, Venkayya VB, Eastep FE. Structural modifications to reduce the LOS-error in large space structures. AIAA 1984:CP-84-0997.
[9] Venkayya VB, Tischler VA. Frequency control and the effect on the dynamic response of flexible structures. AIAA 1984:CP-84-1044.
[10] Grigoriadis KM, Carpenter MJ, Zhu G, Skelton RE. Optimal redesign of linear systems. American control conference; 1993. p.2680–4.
[11] Smith MJ, Grigoriadis KM, Skelton RE. Optimal mix of passive and active control in structures. J Guidance Control Dyn 1992;15(4):912–9.
[12] Onoda J, Haftka RT. An approach to structure/control simultaneous optimization for large flexible spacecraft. AIAA 1987;25(8):1133–8.
[13] Rao SS. Combined structural and controller optimization of flexible structures. Eng Opt 1998;13(1):1–16.
[14] Salama M, Hamidi M, Demsetz L. Optimization of controlled structures. Proc Jet Prop Workshop Identif Control Flexible Space Struct. San Diego, CA; 1984. p. 311–7.
[15] Miller DF, Shim J. Combined structural and control optimization for flexible systems using gradient based searches. AIAA 1986:CP-86-0178.
[16] Khot NS. Structures/control optimization to improve the dynamic response of space structures. Comp Mech 1988;3:179–86.
[17] Rao SS. Combined structural and control optimization of flexible structures. Eng Optim 1988;13:1–16.
[18] Fathy HK, Reyer JA, Papalambros PY, Ulsoy AG. On the coupling between the plant and controller optimization problems. Proc American Control Conf; 2001.
[19] Curadelli RO, Riera JD. Reliability based assessment of the effectiveness of metallic dampers in buildings under seismic excitations. Eng Struct 2004;26:1931–8.
[20] Dyke SJ. Acceleration feedback control strategies for active and semi-active systems: modeling, algorithm development and experimental verification. Ph.D. dissertation, at the University of Notre Dame, IN; 1996.
[21] Tzan SR, Pantelides CP. Convex model for seismic design of structures. II: Design of conventional and active structures. Earth Eng Struct Dyn 1996;25:945–63.
[22] Salama M, Garba J, Demesetz L. Simultaneous optimization of controlled structures. Comp Mech 1988;3:275–82.
[23] Chattopahyay A, Seeley CE. Multiobjective design optimization procedure for control of structures using piezoelectric materials. J Intell Mater Syst Struct 1994;5:403–11.
[24] Cheng FY, Li D. Multiobjective optimization of structures with and without control. J Guide Control Dyn 1996;19(2):392–7.
[25] Rao SS, Venkayya VB, Khot NS. Game theory approach for the integrated design of structures and controls. AIAA 1988;26(4):463–9.
[26] Khot NS. Multicriteria optimization for design of structures with active control. J Aerosp Eng 1998;112:45–51.
[27] Cimellaro GP, Soong TT, Reinhorn AM. Integrated design of controlled linear structural systems. J Struct Eng 2009;135(7):853–62.
[28] Cimellaro GP, Soong TT, Reinhorn AM. Integrated design of inelastic controlled structural systems. Struct Control Health Monit 2009;16:689–702.
[29] Takewaki I. An approach to stiffness-damping simultaneous optimization. Comput Meth Appl Mech Eng 2000;189:641–50.
[30] Park K-S, Koh H-M, Hahm D. Integrated optimum design of viscoelastically damped structural systems. Eng Struct 2004;26:581–91.
[31] Cimellaro GP. Simultaneous stiffness-damping optimization of structures with respect to acceleration, displacement and base shear. Eng Struct 2007;29:2853–70.
[32] Ribakov Y, Gluck J. Optimal design of ADAS damped MDOF structures. Earthq Spectra 1999;15(2):317–30.
[33] Schenauer H, Koski J, Osyczka A. Multicriteria design optimization: procedures and applications. Springer-Verlag; 1990.
[34] Szidarouszky F, Gershon ME, Duckstein L. Techniques for multiobjective design making in systems management. NY: Elsevier Science; 1986.
[35] Khot NS, Oz H, Grandhi RV, Eastep FE, Venkayya VB. Optimal structural design with control gain norm constraint. AIAA J 1988;26(5):604–11.
[36] Soong TT, Grigoriu M. Random vibration of mechanical and structural systems. New Jersey: Prentice Hall; 1993.
[37] Vanmarcke EH. Structural response to earthquakes. In: Lomnitz C, Rosenblueth E, editors. Seismic risk and engineering decisions. Amsterdam: Elsevier; 1976.
[38] Giaralis A, Spanos PD. Effective linear damping and stiffness coefficients of non-linear systems for design spectrum based analysis. Soil Dyn Earthq Eng 2010;30:798–810.
[39] Clough RW, Penzien J. Dynamics of structures. 2nd ed. NY: Mc-Graw Hill; 1993.
[40] De la Fuente E. An efficient procedure to obtain exact solutions in random vibration analysis of linear structures. Eng Struct 2008;30:2981–90.
[41] Der Kiureghian A. Structural response to stationary excitation. J Eng Mech Div ASCE 1980;106:1195–213.
[42] Bertero V, Mahin S, Herrera R. Aseismic design implications of near-fault San Fernando earthquake records. Earth Eng Struct Dyn 1978;6:31–42.
[43] U.B.C. Uniform building code; 1997. p. 1–3.